JOURNAL OF MATERIALS SCIENCE 30 (1995) 3307–3318

The morphology, chain structure and fracture behaviour of high-density polyethylene

Part I *Fracture at a constant rate of deflection*

B. J. EGAN, O. DELATYCKI
Department of Mechanical and Manufacturing Engineering, University of Melbourne, Parkville, Victoria 3052, Australia

The fracture behaviour of high-density polyethylene has only recently become the subject of comprehensive studies. Few of these studies have utilized a group of resins with systematic variation in molecular properties. In this work, a series of samples with controlled variation in chain structure have been prepared using commercial polymerization facilities. The fracture behaviour of these samples has been measured at both a constant rate of deflection and in static fatigue. Comprehensive statistical techniques were used to correlate these fracture results with the chain structure and morphology of the samples. Part I of this work presents the results for the work conducted at a constant rate of deflection. Both the fracture toughness and crack-growth rate were found to be most strongly dependent on the molecular weight of the resin. This is not an unexpected result. However, when variations in molecular weight are minimal, it was found that increasing the short branch content offers considerable scope for improving the fracture performance. Furthermore, longer short branches were found to be more effective at enhancing fracture behaviour. These results, which are of significant commercial importance, are interpreted in terms of existing models for the fracture process in polyethylene.

1. Introduction

High-density polyethylene (HDPE) is being used increasingly as an engineering material. An example of this is the use of HDPE pipes for the distribution of water and gas. In these applications the long-term performance and reliability of the pipes are critical. In order to optimize the lifetime of such pipes it is important to have a comprehensive understanding of the fracture properties of HDPE.

The mechanical strength of HDPE, and indeed of other polymeric materials, is influenced by a large number of parameters. A simplistic representation of these parameters is presented in Fig. 1. Although this diagram is by no means intended to be exhaustive, it serves as a useful illustration of the complexity involved in understanding the mechanical performance of HDPE. Clearly, to include all these parameters in a single study would be a near impossible task. To simplify matters the processing conditions (Box B, Fig. 1) were not varied during this study. The test temperature and test environment were also held constant.

Two distinct sets of parameters remain. One is the chain structure, represented by Box A. The other group of variables, shown in Box C, describe the morphology of the material. Molecular weight and branching (Box A) can influence the fracture behaviour of polyethylene (Box D) directly through the concentration of inter-crystalline links. An indirect mechanism by which these parameters can effect the fracture behaviour is by their influence on the morphology of HDPE (Box C).

The strong dependence of the fracture behaviour of HDPE on molecular weight is well documented [1–5]. Some grades of HDPE contain a small number of short branches arising from the incorporation of 1-olefin comonomer during polymerization. Bubek and Baker [6] have reported improved environmental stress cracking resistance in HDPE resins manufactured using a comonomer. Lu *et al.* [7] have also found the resistance to static fatigue to be greater in an ethylene 1-hexene copolymer than in a straight homopolymer. However, a systematic study of the influence of short branch concentration on fracture behaviour has not been conducted. It is for this reason that, in this research project, particular emphasis was placed on elucidating the effect of short branches on the fracture behaviour of high-density polyethylene.

The chain structure and morphology of a series of eleven HDPE resins have been comprehensively characterized using a range of analytical techniques. The fracture resistance has been measured at both a constant rate of deflection and in static fatigue. This fracture testing was performed using the double

0022–2461

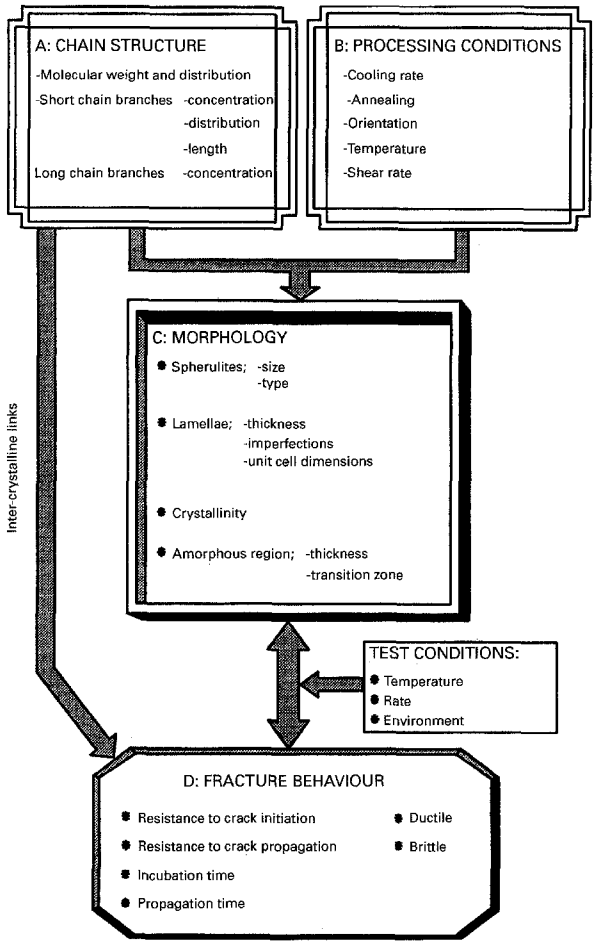

Figure 1 Overview of how a large number of parameters interact to determine the fracture behaviour of HDPE.

torsion fracture geometry, which has previously been shown to generate valid fracture results for HDPE [8]. The advantage of this technique is that it allows information to be collected for both crack initiation and crack growth. A comprehensive statistical analysis has been used to determine those structural and morphological parameters that control the resistance to crack initiation and crack propagation. A similar approach has been successfully applied to understanding the inter-relationship between morphology and mechanical properties in polyamide 6 [9].

The role of each parameter identified by the statistical model as significantly influencing fracture behaviour will be rationalized in terms of the Friedrich [10] model of fracture in polyethylene. In this paper the data of tests performed at a constant rate of deflection will be considered. A subsequent publication will present the findings of the static fatigue analysis.

2. Experimental procedure

2.1. Material

Previous systematic studies of the relationship between fracture toughness, chain structure and morphology have either used narrow molecular weight distribution fractions [2], or a range of whole polymers with widely varying characteristics [1]. Results obtained using essentially monodisperse fractions cannot be applied with confidence to commercial resins that have a broad molecular weight distribution. On the other hand, simultaneous variation of a number of chain parameters may obscure some of the correlations between polymer structure and fracture behaviour.

To avoid these complications, a series of whole polymers has been specially manufactured using commercial polymerization facilities. During the production of a single grade of resin the reactor conditions were varied slightly, with the aim of producing samples of similar molecular weight distribution, but varying short branch content. A controlled variation in chain structure was achieved. This has allowed the development of a better understanding of the influence of chain structure on the fracture behaviour of HDPE.

2.2. Chain structure and morphology

A total of nine ethylene 1-butene high-density resins was produced (samples A–I). These samples allowed the analysis of the influence of short branch concentration on fracture behaviour. Another important parameter is the short branch length. To understand how this parameter effects fracture resistance, two ethylene 1-hexene comonomers were sourced from another production facility (samples J and K). The chain structure and morphology of all eleven resins have been thoroughly characterized.

2.2.1. Molecular weight

Molecular weights were characterized using a Waters gel permeation chromatograph type 150-C ALC/GPC, operated at 140 °C with a flow rate of 1.0 ml min^{-1}. A linear ultrastyragel column was used. The elution solvent was 1,2-dichlorobenzene. Samples were prepared from the polyethylene pellets at 0.25% wt/vol, and were stabilized with 0.03% wt/vol Topanol. The injection volume was 50 μl.

Narrow distribution polystyrene standards were used to calibrate the column. Polystyrene equivalent molecular weights were later adjusted to polyethylene values using conversion factors calculated for NBS polyethylene standards. The number average, $\bar{M}_n$, and weight average, $\bar{M}_w$, molecular weights are listed in Table I.

2.2.2. Degree of short chain branching

Nuclear magnetic resonance (NMR) spectra were accumulated on a Varian Gemini 200 spectrometer fitted with a variable temperature controller. The operating frequency for ^{13}C was 50.1 MHz. Samples for NMR analysis were cut from fracture specimens. These were placed in 5 mm o.d. tubes and dissolved at 20% wt/wt in 1,2,4-trichlorobenzene. Following Bugada and Rudin [11], the specimens were heated at 160 °C for a short time prior to analysis. This destroys all remnants of crystallinity. Between 4000 and 6000 scans were accumulated for each sample at 115 °C. A total recycle time of 3 s with a 30° (8.0 μs) pulse width was used. The field homogeneity was good, and so no lock was used.

TABLE I Summary of experimental data characterizing the chain structure and morphology of the HDPE copolymers used in this work. Only variables for which significant variation occurred between the samples are listed

Sample	Comonomer type	$\bar{M}_n$ (10^4 Dalton)	$\bar{M}_w$ (10^5 Dalton)	Short branches/ 1000C	X_c (%)	L_c nm	L_a nm
A	1-butene	1.03 ± 0.03	1.30 ± 0.04	1.3 ± 0.1	73.93 ± 0.02	21.2 ± 1.0	11.2 ± 0.5
B	1-butene	1.00 ± 0.03	1.29 ± 0.04	1.9 ± 0.1	72.21 ± 0.06	19.9 ± 0.6	11.2 ± 0.3
C	1-butene	0.94 ± 0.03	1.24 ± 0.04	2.0 ± 0.1	72.46 ± 0.02	19.9 ± 0.2	11.2 ± 0.1
D	1-butene	0.94 ± 0.03	1.23 ± 0.04	1.1 ± 0.1	75.89 ± 0.04	22.3 ± 0.7	11.3 ± 0.3
E	1-butene	0.96 ± 0.03	1.33 ± 0.04	2.3 ± 0.1	72.09 ± 0.04	19.5 ± 0.1	11.1 ± 0.1
F	1-butene	1.07 ± 0.03	1.32 ± 0.04	3.2 ± 0.2	70.68 ± 0.06	18.1 ± 0.1	11.4 ± 0.1
G	1-butene	1.17 ± 0.04	1.39 ± 0.04	3.1 ± 0.2	71.32 ± 0.02	18.4 ± 0.2	11.6 ± 0.1
H	1-butene	1.08 ± 0.03	1.36 ± 0.04	2.7 ± 0.1	71.19 ± 0.08	17.9 ± 0.5	11.0 ± 0.3
I	1-butene	1.45 ± 0.04	1.53 ± 0.05	1.4 ± 0.1	72.21 ± 0.04	20.2 ± 0.3	12.2 ± 0.2
J	1-hexene	1.47 ± 0.04	1.01 ± 0.03	2.0 ± 0.1	71.19 ± 0.06	17.4 ± 0.7	11.8 ± 0.5
K	1-hexene	1.35 ± 0.04	1.90 ± 0.03	0.9 ± 0.1	76.83 ± 0.04	22.4 ± 0.3	10.3 ± 0.1

Peak areas were determined using a Planix 5000 digitizing planimeter. Branch concentration is calculated as branches per 1000 structural carbons by obtaining the ratio of individual peak areas against the total area. The results presented in Table I are averages of values obtained from a number of the peaks associated with each branch type.

2.2.3. Crystallinity

The weight fraction of crystallinity, X_c, is calculated from the density according to Equation 1 [12–14]. Here ρ_a is the density of the amorphous phase, ρ_c is the density of the crystalline phase, and ρ is the bulk sample density. The values of ρ_a and ρ_c were taken as 0.853 and 1.000 g cm^{-3}, respectively [15]. Bulk sample densities were measured according to ASTM test method D792 [16]. The measured values of X_c are included in Table I.

$$X_c = \frac{\rho_c(\rho - \rho_a)}{\rho(\rho_c - \rho_a)} \quad (1)$$

The crystalline fraction of each sample was also measured using differential scanning calorimetry and wide-angle X-ray diffraction. The absolute value obtained by each method is different. This disparity between methods is due to the fact that each technique measures a different property to determine the crystallinity. However, each method showed a similar trend in the values of crystallinity across the samples. The crystallinity measured by density was found to be the most reproducible, and so these values will be considered for the statistical analysis.

2.2.4. Crystal and amorphous thickness

Small-angle X-ray analysis (SAXS) was used to determine the thickness of the crystalline and amorphous domains. The small-angle X-ray scatter was measured using an Anton Paar Kratky camera connected to a Philips PW1373/00 goniometer supply unit. A Cu(Ni) radiation source operating at 40 kV and 25 mA was used ($\lambda = 0.154$ nm). Entrance and exit slit widths were set at 100 μm. Scattered intensities were measured by a scintillation counter with a pulse height analyser. This was interfaced to a computer, which stored the data for subsequent analysis.

SAXS spectra were recorded in the step scanning mode. A step size of 50 μm was used through the major peak. X-ray samples 1.5 mm thick were machined from the fracture specimens and tested in triplicate. The position of the main beam was determined by removing the sample and step scanning at 50 μm through the primary radiation. This position was taken as the zero angle in structural calculations.

Slit desmearing was performed according to the procedure developed by Schmidt and co-workers [17–19]. After desmearing, the Lorentz correction was applied [20, 21]. Peak positions were determined by fitting a parabola to eleven points about the primary maxima. Bragg's law [22] was used to calculate the long period, L_{ca}, from these peak positions. The average crystal size was calculated from the long period using Equation 2 [20, 23]. The amorphous thickness, L_a, is determined by difference. Values of L_c and L_a are reported in Table I.

$$L_c = L_{ca} X_c \frac{\rho}{\rho_c} \quad (2)$$

The crystal thickness values were also measured by differential scanning calorimetry (DSC) following Wlochowicz and Eder [24]. The DSC values were consistently lower, but a similar trend in crystal thickness was observed. This confirms the reliability of the small-angle X-ray data. The X-ray values of L_c were determined with smaller experimental errors, and so these values were used for the statistical analysis.

2.2.5. Other structural and morphological parameters

As well as the parameters listed above, several other properties were measured during the characterization of the resin samples. These included degree of unsaturations, number of long chain branches, unit cell dimensions, transition zone thickness, spherulite size and the mean microstrain (or distortion) of the crystals. These values are not reported here, because there was no significant difference between the samples for

any of these parameters. As such, they were not included in the statistical model.

2.3. Fracture analysis

2.3.1. Fracture parameters

Fracture measurements were made using the double torsion fracture geometry. The specimen preparation technique and experimental methodology used to test HDPE in this geometry have been reported previously [8]. Double torsion was chosen as the test geometry because it allows easy measurement of crack propagation parameters as well as crack initiation parameters [25–27].

The resistance to crack initiation is represented by the critical stress intensity factor, K_{Ic}. This is calculated according to Equation 3 [28]

$$K_{Ic} = P W_m \left[\frac{3}{W d^3 d_n (1-\nu)\xi}\right]^{1/2} \quad (3)$$

where ν is Poisson's ratio of the test material, ξ is a function of the specimen width and thickness, P is the load at crack initiation, and W, W_m, d and d_n are various specimen dimensions as defined in Fig. 2. Following Leevers [29], a large deflection correction was also applied to the stress intensity values reported in this paper.

The resistance to crack propagation can be expressed in terms of the rate of crack growth, $\dot{a}_{crd}$. Here the subscript "crd" indicates that the test was performed at a constant rate of deflection. Crack speeds were measured by vaporizing a metallized grid on to the surface of the fracture specimen. The increase in resistance of the grid is monitored with time. A more detailed description of this procedure is given elsewhere [8].

The crack speeds reported in Table IV are those measured at the crack tip. Owing to the curved shape of the crack in double torsion test pieces (Fig. 3) the crack speed will vary along the crack profile. If the crack shape was to alter from one sample to the next, then the crack-tip velocity would not be a suitable parameter to use in comparing the resistance to crack growth. However, work by the authors has shown that the crack shape remains constant for all samples tested [30]. Thus, for HDPE tested in double torsion, the velocity measured at the tip of the crack is a satisfactory parameter to use when comparing the samples.

2.3.2. Test conditions

In our earlier work it was demonstrated that when HDPE is tested in double torsion, valid fracture results are obtained whenever the ASTM minimum thickness criterion is met [8]. Minimum thickness values calculated from fracture toughness measurements on 11 mm thick specimens are presented in Table II. A crosshead speed of 1 mm min^{-1} was used for all fracture tests reported in this paper.

Chan and Williams [31] have shown that the minimum thickness requirement decreases monotonically

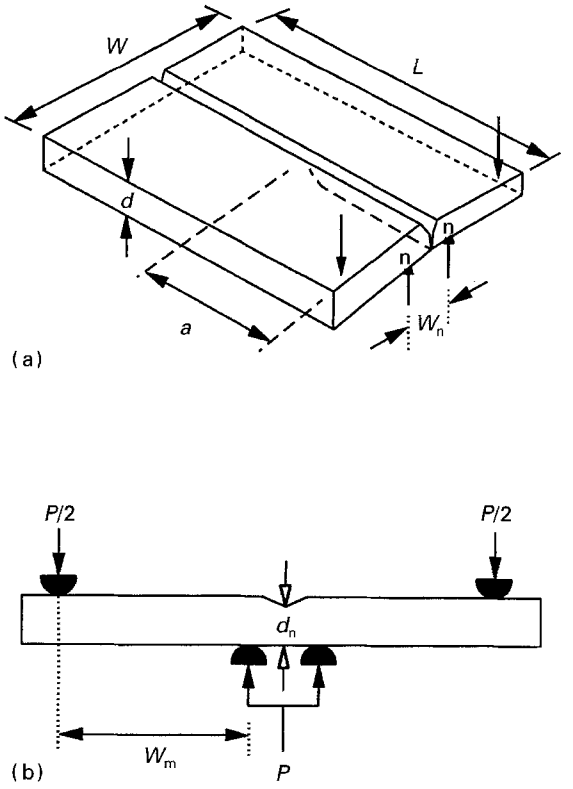

Figure 2 Schematic diagram of the double torsion fracture geometry: (a) perspective view, (b) end view.

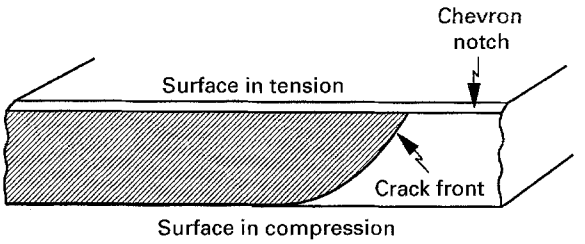

Figure 3 Schematic diagram of the crack profile in double torsion fracture specimens.

TABLE II Minimum thickness criteria, according to ASTM E399, at selected temperatures

Sample	Minimum thickness for plane strain (mm)			
	− 60 °C	− 40 °C	− 20 °C	0 °C
A	–	6.8	7.9	–
B	–	–	7.2	–
C	–	–	6.0	–
D	–	–	6.8	–
E	–	9.9	–	–
F	11.6	13.3	–	–
G	9.4	12.5	–	–
H	–	9.8	–	–
I	27.7	38.6	–	–
J	–	10.2	–	–
K	–	–	3.8	4.5

with temperature. At − 40 °C, only samples F, G and I fail to satisfy the ASTM minimum thickness criterion. To check whether the results for these samples were also measured in plane strain, thinner specimens

TABLE III Comparison of the fracture toughness of samples F and I measured using double torsion specimens of different thicknesses

Thickness d_n(mm)	K_{Ic}(MNm$^{-3/2}$)	
	Sample F	Sample I
11	3.21 ± 0.09	5.38 ± 0.24
7	3.34 ± 0.19	–
6	–	5.61 ± 0.53

of samples F and I were tested. The results are presented in Table III. For both materials, when specimens thinner than 11 mm were tested, a fracture toughness identical to that of the 11 mm thick specimens was obtained. This shows that both sets of results are thickness-independent plane strain values [32]. At − 40 °C, sample G was closer to satisfying the ASTM criterion than samples F or I. Based on the results of the latter materials it is reasonable to assume that 11 mm thick specimens of sample G are also in plane strain.

This analysis shows that at − 40 °C valid fracture measurements for each of the test materials were obtained. All results reported in this paper pertain to data collected at − 40 °C.

2.3.3. Fracture results

Equation 3 contains the Poisson's ration, ν. Only limited data on ν exist for high-density polyethylene [33, 34]. Moreover, there is no information concerning the variation of ν with temperature below 20 °C. It was necessary, therefore, to evaluate Poisson's ratio for HDPE at the test temperature used. For large isotropic samples, ν can be calculated from the relationship between tensile modulus, E, and shear modulus, μ [35, 36]. Within the limits of experimental accuracy, the Poisson's ratio of sample A was found to be invariant and equal to 0.4 over the temperature range 0 °C to − 50 °C. This value was used in all calculations. The corresponding fracture data are listed in Table IV.

3. Statistical analysis

An extensive statistical analysis was used to elucidate the relationship between K_{Ic}, $\dot{a}_{crd}$ and the morphology and chain structure of the HDPE samples. The analysis was performed in terms of three groups of resins. These were samples A–H, samples A–I and samples J and K. Samples A–H exhibit moderate variation in molecular weight, but a three-fold change in short branch content. Analysis of the results for samples A–H will provide insight in to the role of short branches during fracture. Sample I was made with the same catalyst type as samples A–H, but with a catalyst composition that produced a significantly higher molecular weight than the other 1-butene resins. Analysis of the results for samples A–I will allow evaluation of the relative influence of molecular weight and short chain branching on the fracture behaviour of HDPE.

TABLE IV Summary of experimental data characterizing the fracture behaviour of the HDPE copolymers used in this work. Measurements were made at − 40 °C using a crosshead speed of 1 mm min^{-1}

Sample	K_{Ic}(MN m$^{-3/2}$)	$\dot{a}$(mm min^{-1})
A	2.42 ± 0.18	26.7 ± 5.2
B	2.12 ± 0.13	29.7 ± 4.1
C	2.23 ± 0.05	31.3 ± 5.4
D	2.18 ± 0.05	29.3 ± 2.0
E	2.85 ± 0.16	18.1 ± 2.5
F	3.21 ± 0.08	19.6 ± 1.8
G	3.13 ± 0.16	19.0 ± 1.1
H	2.81 ± 0.16	22.6 ± 0.7
I	5.38 ± 0.24	7.1 ± 1.5
J	2.89 ± 0.20	17.4 ± 2.0
K	1.74 ± 0.07	45.2 ± 5.6

Samples J and K are ethylene 1-hexene copolymers. These samples were not included in the statistical analysis, because short branch length is a parameter of the sample and not a numeric variable which can be included in a mathematical model. However, a descriptive analysis of the influence of short branch length will be presented.

3.1. Backward stepwise regression

It was not an aim of this work to arrive at an equation for predicting the fracture characteristics of HDPE resins. The purpose of using a statistical analysis was to screen the parameters $\bar{M}_w$, $\bar{M}_n$, short chain branches (SCB), L_c and L_a to determine which have a significant effect on the fracture behaviour of polyethylene.

Statistical screening of variables in a model can be performed using a number of procedures. The simplest of these is to use a t-test to determine the significance of the individual coefficients generated by a multiple linear regression analysis. However, this procedure is inadequate if there is significant inter-dependence between some of the variables [37]. The complex relationship between chain structure and morphology illustrated in Fig. 1 shows that such inter-dependencies are likely to exist in HDPE. Consequently, a more elaborate screening procedure than the t-test must be used. The procedure chosen was backward stepwise regression, which is capable of taking into account inter-dependence between variables [37]. Initially all the variables are included in the model. The variables are then systematically removed from the model until the only variables remaining are those that make a significant contribution to the quality of fit.

The structural and morphological variables that showed variation in all samples are $\bar{M}_n$, $\bar{M}_w$, SCB, X_c, L_c, and L_a. Equation 2 shows that the crystal thickness, L_c, is calculated from the crystalline fraction, X_c. As such, these two variables are linearly interdependent. Indeed, linear regression between L_c and X_c gives a goodness of fit of $R^2 = 0.94$ for samples A–H, and $R^2 = 0.91$ for samples A–I. Other workers [1, 38] have also observed a strong correlation between crystal thickness and the degree

of crystallinity. Because L_c and X_c are related in this manner, these two parameters are essentially measuring the same property, and so will contribute the same information to the statistical model. To avoid a bias being introduced into the analysis, only one of these variables should be included in the regression model. The aim of this research was to relate fracture behaviour to the micro-structure of the sample. Because the degree of crystallinity is a bulk property, it was chosen as the parameter to be eliminated. The subset of variables to be used in the stepwise regression procedure was, therefore, $\bar{M}_n$, $\bar{M}_w$, SCB, L_c, and L_a.

A backward stepwise regression was performed at the 95% level of significance. The analysis was performed on a PC computer using commercially available statistical software. The final regression model fitter to the fracture data was of the form

$$y = \beta_0 + \beta_1 x_1 + \beta_2 x_2 + \cdots + \beta_n x_n \qquad (4)$$

where the dependent variable y represents a fracture parameter, the independent variables x represent morphological and chain structure parameters, and β_0 is the regression constant. Table V lists the stepwise regression coefficients, β, for the two fracture parameters and two groups of samples analysed. A blank entry in Table V indicates that the variable in question was removed from the model during the stepwise screening procedure. These variables do not significantly influence the corresponding fracture parameter.

3.2. Ridge regression

The coefficients in Table V were calculated under the assumption that the optimum variables are not significantly collinear. A useful measure of the amount of collinearity between variables is given by the sample correlation coefficients, r. The absolute value of r ranges between 0 and 1, with values close to one indicating a high degree of linear dependence. The sample correlation coefficients are conveniently expressed as a correlation matrix. This is shown in Table VI for samples A–H, and Table VII for samples A–I.

Tables VI and VII show that it is invalid to assume all variables in the statistical model are not collinear. Under these circumstances we cannot be confident that the coefficients shown in Table V accurately represent the true value. Because it was not an aim to develop predictive equations for the fracture behaviour of HDPE, the precise value of the individual coefficients are not of primary interest. However, it is important to be confident that the sign of the coefficients is correct. The sign indicates the direction in which the morphology and chain structure parameters influence fracture behaviour. This must be known if the influence of these parameters is to be understood. Because extensive multicollinearity means that we cannot have confidence in the sign of the stepwise regression coefficients, further statistical analysis was required.

A solution to the problem of highly linear dependent variables is to resort to biased estimation techniques [37]. One such procedure is ridge regression. A ridge analysis based on the method of Lagrange multipliers was used. This technique initially sets the regression coefficients equal to the unbiased least squares values. A small amount of bias is gradually introduced into the regression model, causing the ridge coefficients to take on new values. With increasing bias the goodness of fit of the model is reduced, but there is increased confidence in the individual coefficients. The aim is to choose the minimum amount of bias at which the value of every ridge coefficient has stabilized.

Ridge regression does not incorporate a mechanism for screening variables. The ridge analysis was therefore applied to the optimum subsets of variables defined by the stepwise procedure. This is a reasonable step, because the stepwise screening process is able to take account of multicollinearity. A ridge analysis was used simply to give enhanced confidence in the sign of the regression coefficients.

Stepwise regression on the K_{Ic} and $\dot{a}_{crd}$ data of samples A–I indicates that $\bar{M}_w$ is the only significant variable. Multicollinearity cannot occur in a regression model containing a single variable. A ridge regression was not needed for these two data sets. Table VIII lists the ridge coefficients of the remaining two sets of data.

4. Discussion

4.1. Fracture model

In order to interpret the results of the statistical analysis it is necessary to have a descriptive model for the fracture process in polyethylene. A very good model was suggested by Friedrich [10]. This parallels closely the model originally introduced by Peterlin [39, 40]. Recent electron microscopy studies by Thomas and co-workers [41–43] have confirmed the suitability of the Friedrich model for describing fracture in HDPE.

In Friedrich's model the plastic deformation of polyethylene is postulated to occur in three stages. Stage one involves small strains ahead of the crack tip.

TABLE V Coefficients of stepwise regression between the fracture parameters and the structural variables of samples A–H and samples A–I

Fracture parameter	Samples in model	Stepwise regression coefficients, β						
		β_0	$\bar{M}_n(\times 10^{-4})$	$\bar{M}_w(\times 10^{-5})$	SCB	$L_c(\times 10^{-2})$	L_a	R^2
K_{Ic}	A–H	5.74	4.5	–	2.06	8.8	− 0.26	0.98
K_{Ic}	A–I	− 10.7	–	10.0	–	–	–	0.88
$\dot{a}_{crd}$	A–H	107.9	–	− 83.0	− 22.7	− 100.4	2.48	0.98
$\dot{a}_{crd}$	A–I	125.2	–	− 77.0	–	–	–	0.85

TABLE VI Correlation matrix for samples A–H. This matrix shows the degree of collinearity between the various parameters. Numbers closer to 1 indicate a higher level of inter-dependence

	$\bar{M}_n$	$\bar{M}_w$	SCB	L_c	L_a
$\bar{M}_n$	+ 1.00	+ 0.87	+ 0.71	− 0.66	+ 0.60
$\bar{M}_w$	+ 0.87	+ 1.00	+ 0.75	− 0.76	+ 0.25
SCB	+ 0.71	+ 0.75	+ 1.00	− 0.95	+ 0.37
L_c	− 0.66	− 0.76	− 0.95	+ 1.00	− 0.13
L_a	+ 0.60	+ 0.25	+ 0.37	− 0.13	+ 1.00

TABLE VII Correlation matrix for samples A–I. This matrix shows the degree of collinearity between the various parameters. Numbers closer to 1 indicate a higher level of inter-dependence

	$\bar{M}_n$	$\bar{M}_w$	SCB	L_c	L_a
$\bar{M}_n$	+ 1.00	+ 0.96	+ 0.02	− 0.21	+ 0.91
$\bar{M}_w$	+ 0.96	+ 1.00	+ 0.11	− 0.33	+ 0.79
SCB	+ 0.02	+ 0.11	+ 1.00	− 0.93	− 0.14
L_c	− 0.21	− 0.33	− 0.93	+ 1.00	+ 0.04
L_a	+ 0.91	+ 0.79	− 0.14	+ 0.04	+ 1.00

This initial strain is accommodated almost entirely in the rubber-like amorphous regions. Accompanying this is a rotation of stacks of parallel lamellae in the direction of the stress. Molecules involved in intercrystalline links begin to uncoil as they take up the applied stress.

The second stage occurs when the link molecules are subjected to a critical level of stress. At this point taut molecular links generate local stresses at the point of entry into a crystal. Hosemann *et al.* [44] postulate that a polyethylene crystal is composed of a number of segments tilted with respect to one another. These segments are known as mosaic blocks, and the boundaries between the mosaic blocks contain screw dislocations. Owing to these dislocations, the stresses from the taut link molecules induce crystallographic slip in the chain direction. The unfolded molecular sections act as tie chains between connecting mosaic blocks.

Local yielding generates submicroscopic defects at heterogeneities between lamellae [10]. These are referred to as microvoids, because they are much smaller than visible crazes. Owing to their elliptical shape, microvoids concentrate stresses at the void tips. These act on adjacent stacks of lamellae to create further microvoids. Between the microvoids are domains of oriented material known as microfibrils. These consist of alternating phases of crystalline and partially extended amorphous material.

Stage three, which involves drawing out the microfibrils, is the stage in which most energy is absorbed. Fibril extension occurs by chain slippage, stretching of partially relaxed link molecules, and further unfolding of chain segments. These events cause the microfibrils to contract laterally and become highly oriented. This is known as strain hardening. The associated increase in strength allows the fibrils to stabilize a greater volume of voids. At this stage microvoid coalescence occurs, whereby the weaker fibrils fail and the cavities between the remaining fibrils become larger [10, 45]. Void coalescence produces the state of fibrillation known as crazing. This appears as a stress-whitened zone in polyethylene.

Strain-hardened fibrils can elongate by drawing material in to the fibril from the craze surface, as well as by chain slip and molecular alignment. Eventually the fibrils become so highly strained that they fail. When this occurs a crack is said to have initiated. The breakdown of the fibrillar structure can occur by scission of entangled chains, or by the molecules sliding past each other and becoming disentangled [10, 46]. Cleavage of covalent bonds generates radicals which can be detected by electron spin resonance or infrared measurements. Several workers [40, 47, 48] have found that, at moderate strain rates, few radicals are formed during the fracture of polyethylene. This indicates that chain slip is the dominant mechanism in the ultimate failure of polyethylene.

From this model we see that for a crack to grow the fibrils joining the surfaces of a craze must rupture. Fibrils rupture as the link molecules that hold them together become disentangled and slide past each other. If there is a higher density of link molecules, then the applied stress will be transferred more effectively throughout the fibril, and the average stress per tie chain will be lower. Furthermore, each link molecule will be more extensively entwined with other structural elements. These features make chain disentanglement more difficult and so prolong the process of fibril extension prior to rupture. Drawing the fibril to greater lengths requires a higher input of energy, which means that the fracture toughness is enhanced. Thus, samples with a higher density of link molecules (tie chains and entangled loops) will have a greater fracture toughness due to greater restriction of chain disentanglement and more extensive stretching of the fibrils.

4.2. Interpretation of statistical analysis

4.2.1. Crack initiation at a constant rate of deflection

The resistance to crack initiation at a constant rate of deflection was measured by the stress intensity factor,

TABLE VIII Coefficients of the ridge regression performed on those data sets for which multicollinearity existed between the screened variables

Fracture parameter	Samples in model	Ridge regression coefficients, β*						
		β_0^*	$\bar{M}_n(\times 10^{-5})$	$\bar{M}_w(\times 10^{-5})$	SCB$(\times 10^{-1})$	$L_c(\times 10^{-3})$	$L_a(\times 10^{-3})$	R^2
K_{Ic}	A–H	0.39	13.0	–	2.6	− 3.7	9.8	0.76
$\dot{a}_{crd}$	A–H	79.3	–	− 42.0	− 20.7	17.0	22.0	0.68

K_{Ic}. A morphological interpretation of fracture results is more easily made in terms of energy absorption than in terms of stress intensification. K_{Ic} is related to the critical strain energy release rate, G_{Ic}, by the Young's modulus [49, 50]. Literature data indicate that HDPE samples of similar density to the ones used in this study show little variation in Young's modulus [51, 52]. As such, the fracture parameters G_{Ic} and K_{Ic} will show similar trends across the samples. Thus, even though the statistical analysis was performed in terms of K_{Ic}, it is legitimate to discuss the results of this analysis in terms of energy absorption.

4.2.1.1. Samples A–H. The critical stress intensity factor of samples A–H was found to increase with the number average molecular weight (Table VIII). A correlation between fracture toughness and molecular weight has been reported previously [1, 2]. In these studies the fracture toughness was found to depend on the average length of the longer molecules ($\bar{M}_w$ or $\bar{M}_z$), as well as on the polydisperity of the sample. Samples A–H all had a similar molecular weight distribution, and so in this case polydisperity is not expected to be included in the statistical model. Moreover, because of the constant polydispersity, the population of long chains is equally well represented by $\bar{M}_n$ as by $\bar{M}_w$. The fact that $\bar{M}_w$ was eliminated from the model before $\bar{M}_n$ appears to be more a mathematical phenomenon than one of real physical significance.

From Friedrich's model it is clear that a primary determinant of fracture toughness in HDPE is link density. The most important structural parameter controlling the number of links is molecular weight. As the average chain length increases, more tie chains and entangled loops are formed [4, 52]. This accounts for the positive correlation observed between fracture toughness and molecular weight for samples A–H.

The fracture toughness of samples A–H was also found to increase with the degree of short chain ethyl branching. There are two main mechanisms that can explain this effect. Model studies by Lacher *et al.* [53, 54], and Mathur *et al.* [55], have predicted an increase in link density with short branch concentration. This will result in an improvement in fracture toughness. The observed positive correlation between K_{Ic} and short branch concentration is partially accounted for by this mechanism.

Short branches are protrusions along a polyethylene chain. For the link molecules to become disentangled it is necessary that part of each molecule is dragged through crystalline domains. The existence of protrusions along the chain will make this process more difficult. An increased resistance to chain slip causes the fibrils to elongate further, and so increases the amount of energy absorbed during fracture. It is postulated that this mechanism is mainly responsible for the observed increase in fracture toughness with degree of ethyl branching.

Short chain branching will also influence the fracture behaviour of HDPE through changes in the morphology of the sample. An increase in short branch concentration is often accompanied by a decrease in crystal thickness [23, 56–58] and an increase in crystalline distortions [59, 60]. The range of ethyl branching observed for samples A–H was insufficient to induce significant differences in the mean microstrain. No conclusions regarding the role of crystalline distortions in the fracture of HDPE can be drawn from the results of this study.

Samples A–H displayed a considerable range of crystal thicknesses. A negative correlation between fracture toughness and crystal thickness was shown in the statistical analysis. Although the crystal thickness is strongly influenced by the degree of short branching, the mechanism by which crystal thickness influences fracture toughness is different to the mechanism by which short chain branching affects fracture toughness. The yield stress of polyethylene crystals decreases with crystal thickness [61, 62]. For a given level of stress intensity at the crack tip the deformation zone will be larger in samples that contain crystals which yield more easily. This results in fibrillation occurring over a larger volume of material. Fibrils are also able to grow to greater lengths in resins containing thinner crystals. This is partly due to the increased ease of lamellar unfolding, and partly to the increased ease of drawing material into the fibril from its root. Fibrillation over a larger volume, and greater elongation of the fibrils, results in more energy absorption during fracture, and thus a higher fracture toughness. It is postulated that these mechanisms account for the increase in K_{Ic} observed with decreasing crystal thickness.

Earlier it was shown that the crystal thickness and crystallinity are related such that a decrease in L_c correlates with an increase in the total amorphous content. Void nucleation occurs in the amorphous region of HDPE. Friedrich postulated that more voids will nucleate in a sample that contains more amorphous material [10]. If more voids nucleate, then more fibrils are formed, resulting in more energy absorption, and so a higher fracture toughness. The negative correlation between fracture toughness and crystal thickness may, in part, be due to the increase in amorphous content that occurs with a decrease in crystal thickness.

The final parameter that was found to significantly influence the fracture toughness of samples A–H is the amorphous thickness, L_a. Model studies by Lacher *et al.* [63–66] indicate that an increase in amorphous thickness is associated with an increase in the density of inter-crystalline links. This is a reasonable finding. Link molecules traverse the amorphous zone. If more link molecules are present, they must occupy a larger volume to avoid over-crowding, and so the amorphous thickness must increase. The positive correlation observed between fracture toughness and L_a is a consequence of the rise in link density that produces the increase in amorphous thickness.

4.2.1.2. Samples A–I When sample I is introduced in to the statistical model the final result is quite different to that for samples A–H. The weight average molecular weight is found to be the only variable that significantly influences the fracture toughness. A dependence

on molecular weight is expected, because molecular weight is the major parameter influencing the number of inter-crystalline links. The critical result is that the short branch concentration, the crystal thickness, and the amorphous thickness are no longer identified as important parameters.

Sample I has a much higher molecular weight and fracture toughness than samples A–H. However, the degree of ethyl branching, the crystal thickness, and the amorphous thickness are similar in magnitude for all nine resins. As a consequence, the molecular weight of sample I has enormous leverage on the statistical analysis. It appears that this leverage obscures the influence on fracture toughness of SCB, L_c and L_a that was observed for samples A–H.

4.2.2. *Crack speed at a constant rate of deflection*

The speed of crack growth at a fixed rate of deflection, ($\dot{a}_{crd}$), was used to measure the resistance to crack propagation. The lower the crack speed the greater the resistance to crack growth. For both groups of samples the same structural variables identified as controlling fracture toughness were also controlling the resistance to crack propagation. This indicates that, despite the different time scales involved, the same deformation mechanism is operating during both crack initiation and crack propagation.

For a craze to become a propagating crack, it is necessary for the fibrils connecting the surfaces of the craze to rupture. Failure of polyethylene fibrils occurs predominantly by the disentanglement of link molecules. As chain disentanglement becomes more difficult, the fibrils become more cohesive and draw out to greater lengths. This implies that a greater crack opening displacement must be achieved to maintain crack growth. At a fixed crosshead speed the rate at which the crack opens is the same for all samples. If the fibrils must be drawn to greater lengths, fewer fibrils will be broken per unit time at a given crosshead speed. This is tantamount to a reduced crack speed. Thus, an increased difficulty of chain slip results in an enhanced resistance to crack propagation due to a lower rate of fibril failure.

4.2.2.1. Samples A–H. For samples A–H an increase in the resistance to crack growth with increasing molecular weight was observed. It was established above that a higher molecular weight results in an increased number of inter-crystalline links, and in more entanglements per link molecule. Both these features act to retard chain disentanglement. Following the above argument, the increased resistance to crack growth with increasing molecular weight is easily understood.

The density of intercrystalline links also increases with the degree of short chain branching. This partially accounts for the positive correlation between the resistance to crack growth and the short branch concentration. Short branches are protrusions along the polymer molecule. It was postulated above that such protrusions inhibit the ability of chains to slip past each other and to slip through crystalline domains. This is an additional mechanism by which short branches retard fibril separation, and thus crack propagation.

A positive correlation between crack growth resistance and amorphous thickness was observed for samples A–H. Because link molecules occupy space in the amorphous region, the more link molecules present, the greater is the volume of amorphous material. Thus, an increase in amorphous thickness is, in part, a direct consequence of a larger number of link molecules. It was shown above that this will inhibit fibril separation, and thus slow the rate of crack growth. This explains the observed correlation.

The final correlation identified by the statistical analysis was between crack speed and crystal thickness. The resistance to crack propagation was found to be greater in samples containing thinner crystals. This is best understood in terms of the larger deformation zone which results from the lower yield stress of thin crystals. A larger deformation zone means that there will be more fibrils across the width of the crack front. For the purpose of illustration, these fibrils can be imagined to be in series with each other. The more fibrils there are "in series", the smaller the amount that each one will elongate for a given increase in crack opening displacement. This is effectively a crack blunting mechanism. A larger change in crack opening must be achieved before the fibril elongation reaches a critical value and the crack can advance. At a constant rate of deflection this results in the resistance to crack growth increasing as the crystals become thinner.

It was argued above that because thinner crystals yield more easily, the fibrils they form are likely to elongate to greater lengths. Longer fibrils result in an increase in the crack opening required to sustain crack advancement. This is an additional reason why crystal thickness is negatively correlated with crack growth resistance in these tests.

4.2.2.2. Samples A–I. When sample I is introduced into the analysis the resistance to crack propagation is found to be solely dependent on the weight average molecular weight. This result is identical to that observed when sample I was included in the fracture toughness analysis. The explanation of this result for the $\dot{a}_{crd}$ data is exactly the same as was given earlier for the K_{Ic} data.

4.3. Influence of short branch length

Samples J and K contain butyl short branches, whereas the remaining samples contain ethyl short branches. Because only two HDPE resins with butyl branches were tested, a rigorous mathematical treatment of the role of short branch length cannot be made. However, a purely descriptive comparison between results for the two types of copolymer is possible. This analysis was performed using the results for samples D, H, J and K. The relative change in chain structure, measured in terms of $\bar{M}_w$, $\bar{M}_n$ and short

TABLE IX Comparison of properties between butyl branched resins and ethyl branched resins

		Ethyl branched resins			Butyl branched resins		
		Sample D	Sample H	% change D → H	Sample K	Sample J	% change K → J
Chain structure	$\bar{M}_n$ (a.m.u.)	9350	10760	15	13500	14650	9
	$\bar{M}_w$ (a.m.u.)	123100	135900	10	89950	101200	13
	SCB (/1000C)	1.1	2.7	145	0.9	2.0	122
Morphology	L_c (nm)	19.5	17.9	− 8	22.4	17.4	− 22
	L_a (nm)	11.1	11.0	− 1	11.8	10.3	− 15
Fracture behaviour	K_{Ic} ($MN\,m^{-3/2}$)	2.18	2.81	29	1.74	2.89	66
	$\dot{a}_{crd}$ ($mm\,min^{-1}$)	29.3	22.6	− 23	45.2	17.4	− 62

branch concentration, is approximately the same between samples D and H as it is between samples K and J. At the same time, the relative change in morphology and fracture behaviour, although in the same direction, is greater for the 1-hexene copolymers than for the 1-butene copolymers. These results are compared in Table IX.

Earlier it was shown that the crystal thickness of the ethylene 1-butene copolymers was controlled by the degree of ethyl branching. It is reasonable to expect that other types of short branch would have a similar effect. The increase in short branch concentration between samples K and J is approximately the same as between samples D and H. However, the reduction in crystal thickness between the two 1-hexene resins is almost three times that for the 1-butene resins. This suggests that longer short branches are more effective at inhibiting the crystal thickness.

The statistical analysis of the 1-butene copolymers indicates that when the difference in molecular weight of two samples is small, crystal thickness plays an important role in determining the fracture behaviour. A resin in which the crystals are thinner will have a higher fracture toughness. The increase in K_{Ic} between samples K and J is twice that between samples D and H. Because the change in molecular weight and short chain branching are of a similar magnitude within both pairs of samples, this difference can be attributed primarily to the greater influence that the butyl branches had on reducing the crystal thickness. This observation indicates that an increase in short branch concentration will be more effective at enhancing fracture toughness if comonomers with longer side-groups are used.

The increase in resistance to crack propagation, $\dot{a}_{crd}$, was twice as large for the 1-hexene pair than for the 1-butene pair. When variations in molecular weight are minimal, the results for the 1-butene resins showed that the resistance to crack propagation was significantly influenced by crystal thickness. It appears, therefore, that incorporating comonomers with longer side-groups into HDPE resins will increase the resistance to crack propagation.

5. Conclusion

It was shown that molecular weight is clearly the most important parameter controlling the fracture behaviour of HDPE. Such a conclusion is expected. However, significant changes to the molecular weight will dramatically alter the processing properties. This is illustrated by the fact that sample I is marketed as a film-grade resin, whereas samples A–H are pipe-grade materials. The increase in molecular weight that can be achieved without altering the processing properties is minimal. When the permitted variation in molecular weight is restricted, the results for samples A to H indicate that an improvement in fracture toughness can still be achieved by increasing the degree of short chain branching. This improvement is brought about directly through the influence of short chain branching on the link density, as well as indirectly through the influence of short branches on the morphology of polyethylene.

A descriptive analysis of the influence of short branch length was performed. The analysis indicates that for a given concentration of short chain branching the crystal thickness is inhibited more if the branches are longer. Based on the relationship between crystal thickness and fracture behaviour, this shows that an increase in the comonomer content will enhance the performance of HDPE by a greater margin if comonomers with longer side chains are used.

Linear low-density polyethylene (LLDPE) is one example of the use of short chain branching to improve fracture toughness. LLDPE can contain 10–30 times more comonomer than HDPE. Although the fracture toughness is enhanced, the material is also much softer due to the lower crystallinity. This limits the range of applications. For instance, LLDPE would not be suitable for underground pipes, because it would deform too easily. A significant improvement in fracture toughness by adding more comonomer was achieved for samples A–H with minimal change to the crystallinity, and hence stiffness. This is a result that has not previously been reported, and which has important practical ramifications. It shows that, within limits, increasing the short branch content of a grade

of HDPE will result in improved fracture resistance without significantly altering the end use requirements (processability and stiffness) of the resin.

The number of observations included in each statistical model is relatively small. With such a limited number of degrees of freedom it is not possible to be totally confident that the statistical analysis applies to all HDPE samples. However, the results were generated using commercially produced whole polymers. As such, they give a reasonable indication of which structural parameters offer the greatest potential for achieving improvements in the fracture behaviour of commercial HDPE resins. The range of variation of each structural and morphological parameter was also relatively small. As a consequence, it is uncertain how far the observed trends can be extrapolated. Furthermore, this work has not determined the limits of branch length and branch concentration beyond which undesirable changes in other properties begin to occur. However, this study does present several findings that are of significant commercial interest.

References

1. D. BARRY, PhD thesis, University of Melbourne (1986).
2. S. H. CARR, B. CRIST and T. J. MARKS, *Gov. Rep. Announce. Index* **85** (1985) 96.
3. Y. L. HUANG and N. BROWN, *J. Mater. Sci* **23** (1988) 3648.
4. A. LUSTIGER and R. L. MARKHAM, *Polymer* **24** (1983) 1647.
5. R. POPLI and L. MANDELKERN, *J. Polym. Sci. Part B Polym. Phys. Ed.* **25** (1987) 441.
6. R. A. BUBEK and H. M. BAKER, in "Abstracts of papers for the Plastics and Rubber Institute 5th International Conference on Deformation, Yield and Fracture of Polymers", Cambridge, 1982, p. 31.1.
7. X. LU, X. WANG and N. BROWN, *J Mater. Sci.* **23** (1988) 643.
8. B. J. EGAN and O. DELATYCKI, *ibid.*, **29** (1994) 6026.
9. J. MAROSFALVI, G. BODOR and W. WILKE, *Kunststoffe* **80** (1990) 93.
10. K. FRIEDRICH, *Adv. Polym. Sci.* **52-53** (1983) 225.
11. D. C. BUGADA and A. RUDIN, *Eur. Polym. J.* **23** (1987) 809.
12. L. E. ALEXANDER, "X-Ray Diffraction Methods in Polymer Science" (Wiley, New York, 1969) p. 189.
13. C. FRANCE, P. J. HENDRA, W. F. MADDAMS and H. A. WILLIS, *Polymer* **28** (1987) 710.
14. G. ALLEGRA, P. CORRADINI, H.-G. ELIAS, P. H. GEIL, H. D. KEITH and B. WUNDERLICH, *Pure Appl. Chem.* **61** (1989) 769.
15. M. J. RICHARDSON, P. J. FLORY and J. B. JACKSON, *Polymer* **4** (1963) 221.
16. ASTM D 792-86, "Standard Test Method for Specific Gravity and Density of Plastics by Displacement" (American Society for Testing and Materials, Philadelphia, PA, 1986).
17. R. W. HENDRICKS and P. W. SCHMIDT, *Acta. Phys. Austriaca* **37** (1973) 20.
18. P. W. SCHMIDT, *Acta. Crystallogr.* **19** (1965) 938.
19. P. W. SCHMIDT and R. HIGHT, *ibid.* **13** (1960) 480.
20. D. S. BROWN and R. E. WETTON, in "Developments in Polymer Characterization", Vol.1 edited by J.V. Dawkins (Applied Science London, 1978) 157.
21. C. G. VONK, "Small Angle X-Ray Scattering", edited by O. Glatter and O. Kratky (Academic Press, London, 1982) p. 433.
22. W. L. BRAGG, *Cambridge Philos. Soc. Proc.* **17** (1913) 43.
23. F. J. BALTÁ CALLEJA, J. C. GONZÁLEZ ORTEGA and J. MARTINEZ DE SALAZAR, *Polymer* **19** (1978) 1094.
24. A. WLOCHOWICZ and M. EDER, *Polymer* **25** (1984) 1268.
25. R. FRASSINE, T. RICCÒ, M. RINK and A. PAVAN, *J. Mater. Sci.* **23** (1988) 4027.
26. J. A. KIES and B. J. CLARK, in "Proceedings of the 2nd International Conference on Fracture", Brighton, 1969, edited by P. L. Pratt (Chapman and Hall, London, 1969) p. 483.
27. J.-C. POLLET and S. J. BURNS, *J. Am. Ceram. Soc.* **62** (1979) 426.
28. B. J. PLETKA, E. R. FULLER and B. G. KOEPKE, in "Fracture Mechanics Applied to Brittle Materials", ASTM STP 678 edited by S.W. Freiman (American Society for Testing and Materials, Philadelphia, PA, 1979) p. 19.
29. P. S. LEEVERS, *J. Mater. Sci. Lett.* **5** (1986) 191.
30. B. J. EGAN and O. DELATYCKI, *ibid.*, **14** (1995) 340.
31. M. K. V. CHAN and J. G. WILLIAMS, *Polym. Eng. Sci.* **21** (1981) 1019.
32. W. F. BROWN and J. E. SRAWLEY, in "Plane Strain Crack Toughness Testing of High Strength Metallic Materials", ASTM STP 410, edited by W.F. Brown, J.E. Srawley (American Society for Testing and Materials, Philadelphia, PA, 1967) p. 1.
33. W. P. LEUNG, C. L. CHOY, C. XU, Z. QI and R. WU, *J. Appl. Polym. Sci.* **36** (1988) 1305.
34. G. SCHENKEL, *Kunststoffe* **63** (1973) 149.
35. ASTM E 132-86 "Standard Test Method for Poisson's Ratio at Room Temperature" (American Society for Testing and Materials, Philadelphia, PA, 1986).
36. C. L. BAUER and R. J. FARRIS, *Polym. Eng. Sci.* **29** (1989) 1107.
37. R. E. WALPOLE and R. H. MYERS, "Probability and Statistics for Engineers and Scientists", 2nd Edn (Collier MacMillan, New York, 1978).
38. C. G. VONK and A. P. PIJPERS, *J. Polym. Sci. Polym. Phys. Ed.* **23** (1985) 2517.
39. A. PETERLIN, *J. Mater. Sci.* **6** (1971) 490.
40. *Idem, J. Phys. Chem.* **75** (1971) 3921.
41. W. W. ADAMS, D. YANG and E. L. THOMAS, *J. Mater. Sci.* **21** (1986) 2239.
42. J. M. BRADY and E. L. THOMAS, *ibid.* **24** (1989) 3311.
43. *Idem, ibid.* **24** (1989) 3319.
44. R. HOSEMANN, W. WILKE and F. J. BALTÁ CALLEJA, *Acta. Crystallogr.* **21** (1966) 118.
45. E. H. ANDREWS and P. E. REED, *Adv. Polym. Sci.* **27** (1978) 3.
46. S. K. BHATTACHARYA, K. SWAPAN and N. BROWN, *J. Mater. Sci.* **19** (1984) 2519.
47. H. GLEITER, *Mater. Forum* **11** (1988) 140.
48. C. L. HAMMOND, P. J. HENDRA, B. G. LATOR, W. F. MADDAMS and H. A. WILLIS, *Polymer* **29** (1988) 49.
49. A. J. KINLOCH and R. J. YOUNG, "Fracture Behaviour of Polymers" (Applied Science, London, 1983).
50. J. G. WILLIAMS, "Fracture Mechanics of Polymers" (Ellis Horwood, Chichester, 1984).
51. B. CRIST, C. J. FISHER and P. R. HOWARD, *Macromolecules* **22** (1989) 1709.
52. L. MANDELKERN and A. J. PEACOCK, in "Proceedings of an International Course and Conference on the Interfaces between Mathematics, Chemistry and Computer Science", Dubrovnik, 1987, edited by R. C. Lacher (Elsevier Applied Science, New York, 1988) p. 201.
53. R. C. LACHER, in "Abstracts of Papers for the 197th ACS National Meeting", Dallas, 1989, Paper 138.
54. *Idem*, in "Proceedings of an International Course and Conference on the Interfaces between Mathematics, Chemistry and Computer Science", Dubrovnik, 1987, edited by R.C. Lacher (Elsevier Applied Science, New York, 1988) p. 235.
55. S. C. MATHUR, K. RODRIGUES and W. L. MATTICE, *Macromolecules* **22** (1989) 2781.
56. R. ALAMO and L. MANDELKERN, *ibid.* **22** (1989) 1273.
57. F. ANIA, H. G. KILIAN and F. J. BALTÁ CALLEJA, *J. Mater. Sci. Lett.* **5** (1986) 1183.
58. G. BODOR, H. J. DALCOLMO and O.SCHRÖTER, *Coll. Polym. Sci.* **267** (1989) 480.
59. U. W. GEDDE, J.-F. JANSSON, G. LILJENSTRÖM, S. EKLUND, S. R. HOLDING , P.-L. WANG and P.-E. WERNER, *Polym. Eng. Sci.* **28** (1988) 1289.

60. P. R. HOWARD and B. CRIST, *J. Polym. Sci. Part B: Polym. Phys. Ed.* **27** (1989) 2269.
61. R. J. YOUNG, *Mater. Forum* **11** (1988) 210.
62. *Idem, Philos. Mag.* **30** (1974) 85.
63. R. C. LACHER, J. L. BRYANT and L. N. HOWARD, *J. Chem. Phys.* **85** (1986) 6147.
64. R. C. LACHER, J. L. BRYANT, L. N. HOWARD and D. W. SUMNERS, *macromolecules* **19** (1986) 2639.
65. R. C. LACHER, *ibid.* **20** (1987) 3054.
66. *Idem, Polym. Preprints* **28** (1987) 268.

Received 30 June 1994
and accepted 20 January 1995